Coupled nutricline and productivity variations during the Pliocene in the western Pacific warm pool and their paleoceanographic implications

Jiangnan Shi [a, e], Qi Jia [b], Dirk Nürnberg [c], Tiegang Li [b, d, *], Zhifang Xiong [b, d], Bingbin Qin [b]

[a] *Key Laboratory of Marine Geology and Environment, Institute of Oceanology, Chinese Academy of Sciences, Qingdao 266071, China*
[b] *Key Laboratory of Marine Geology and Metallogeny, First Institute of Oceanography, Ministry of Natural Resources, Qingdao 266061, China*
[c] *GEOMAR Helmholtz Center for Ocean Research Kiel, Wischhofstrasse 1–3, Kiel 24148, Germany*
[d] *Laboratory for Marine Geology, Qingdao National Laboratory for Marine Science and Technology, Qingdao 266237, China*
[e] *University of Chinese Academy of Sciences, Beijing 100049, China*

ARTICLE INFO

ABSTRACT

The tropical Pacific played an important role in modulating global climate change during the Pliocene. Studies of tropical Pacific sea surface temperatures covering the period from the Pliocene onwards indicate that changes in the thermal mean state over the tropical Pacific can significantly influence global climate feedbacks and connect the high- and low-latitude climates. Tropical productivity fluctuations are a significant mechanism with respect to the operation of the global carbon cycle. Yet, temporal changes in primary productivity are not well constrained in the western Pacific warm pool (WPWP), where the ocean–climate system is not dominated by upwelling systems. Furthermore, the role of nutricline dynamics in forcing productivity over tectonic timescales remains uncertain. Here we use relatively high-resolution foraminiferal carbon isotope records combined with Ba/Ti ratios obtained from International Ocean Discovery Program (IODP) Site U1490 in the WPWP to reconstruct nutricline depth and paleoproductivity over the period 5.1–2.6 Ma. Our records imply that nutricline and productivity variations were closely coupled over tectonic timescales, implying that the dynamics of the nutricline play a significant role in regulating productivity in the WPWP. The deeper nutricline and lower productivity during 4.8–3.5 Ma might have been fostered by the closure of the Central American Seaway through the thickening of the mixed layer in the WPWP. We relate the overall shallower nutricline and increased productivity during 3.5–3.0 Ma to the restriction of the Indonesian Seaway via the enhanced influence and upwelling of high-latitude southern-source waters.

1. Introduction

Several significant climate events occurred during the Pliocene (~5.3–2.6 Ma), including the Pliocene warm period (ca. 5.0 Ma to 3.0 Ma) and the intensification of the Northern Hemisphere glaciation (iNHG; ca. 2.75 Ma; Ravelo et al., 2004). In addition, it was a critical period during which two important low-latitude tectonic events, the closure of the Central American Seaway (CAS) and the constriction of the Indonesian Seaway (ITF), effectively changed the global oceanic circulation and hence altered the distribution of heat between basins (Driscoll and Haug, 1998; Haug and Tiedemann, 1998; Cane and Molnar, 2001; Karas et al., 2009, 2011). The tropical Pacific between these two seaways provides substantial amounts of the global atmospheric sensible and latent heat, and water vapor and thus, plays an important role in driving climate change (Wara et al., 2005).

As is the largest reservoir of warm surface water on Earth, in particular the Western Pacific Warm Pool (WPWP) contributes to the planetary-scale atmospheric circulation (Yan et al., 1992). As the WPWP has a profound impact on the global heat budget, as well as the hydrological, carbon, and biogeochemical cycles, small variations in the mean climatic state over the tropical Pacific significantly affect regional hydrological features (Hoerling et al., 2001). At present, the general climatic patterns across the WPWP are characterized by El Niño-Southern Oscillation (ENSO) variations (Fedorov and Philander, 2000), the Walker and Hadley circulations, and latitudinal shifts in the Intertropical Convergence Zone (ITCZ; Schneider et al., 2014). The WPWP, as part of the Indo-Pacific warm pool, is not only connected to the eastern

tropical Pacific (ETP; Picaut et al., 1996), but also exchanges water with the Indian Ocean through the Indonesian Seaway (Lukas et al., 1996).

In view of the importance of the modern WPWP to global climate change, many studies showed that the WPWP changed significantly during the Pliocene (e.g., Bali et al., 2020; Brierley et al., 2009; Ford et al., 2015; Ford and Ravelo, 2019; Li et al., 2011; Wara et al., 2005). An expanded warm pool was proposed by the evidence that the meridional thermal gradient was reduced during the early Pliocene (Brierley et al., 2009). In addition, previous reconstructions suggest that the Pliocene zonal sea surface temperature (SST) gradient and the thermocline tilt along the equator was weaker in comparison to modern conditions, which is referred to as a quasi permanent El Niño-like state (Brierley et al., 2015; Chaisson and Ravelo, 2000; Fedorov et al., 2006, 2010; Ravelo et al., 2014; Wara et al., 2005). Vertical temperature gradients further indicate that the El Niño-like conditions included a warm/deep thermocline not only in the ETP but also across the entire tropical Pacific (Ford et al., 2012, 2015). After ~4 Ma, the tropical thermocline cooled/shoaled as the global climate gradually transferred towards the cooler Pleistocene (Ford et al., 2015). These changes in the upper ocean structure as well as nutrient distributions of the tropical Pacific were partly related to the closing/constriction of the CAS and the ITF (Auer et al., 2019; Bali et al., 2020; Ford et al., 2012; Kamikuri et al., 2009; Steph et al., 2010).

Only a few studies have focused on the interrelationship between marine productivity and nutricline dynamics (the latter being an ocean layer in which there is a rapid change in nutrient content with depth) in the western tropical Pacific (WTP) during the Pliocene. During modern El Niño events, surface currents along the equatorial Pacific are impeded by the weakened trade winds (McPhaden et al., 2006; Sagawa et al., 2012). This results in a lifting of the thermocline and the nutricline and thus increased primary productivity in the WTP (Williams and Grottoli, 2010). However, studies related to the past ENSO-like influences on biogeochemical cycles have concentrated on the ETP (Drury et al., 2018; Kamikuri et al., 2009; Lyle et al., 2019; Lyle and Baldauf, 2015). Consequently, the dynamics of the WTP and its role in biogeochemical cycling during the Pliocene remain poorly understood although highly relevant as the Pliocene was a period during which the boundary conditions were rather similar to those of today. Whether a covariant relationship existed between the nutricline and productivity during the Pliocene epoch, and whether ENSO-like fluctuations played a role in productivity changes in the Pliocene WTP, remain rather unclear.

To address these issues, we here present a long-term Pliocene record of foraminiferal stable carbon isotopes ($\delta^{13}C$) and bulk Ba/Ti ratios obtained from International Ocean Discovery Program (IODP) Site U1490 in the central WPWP. We analyzed 302 samples for $\delta^{13}C$ measurements on each of the 3 foraminifera species (*Trilobatus sacculifer*, *Globorotalia tumida* and *Cibicidoides wuellerstorfi*) and 565 samples for Ba/Ti analyses on bulk sediments to reconstruct nutricline depth and productivity changes and their possible response to tectonic events over the period 5.1–2.6 Ma. Consequently, these new datasets allowed to evaluate the possible forcing mechanisms associated with variations in nutricline depth and productivity in the WPWP over tectonic timescales.

2. Regional setting

Site U1490 is located in the WPWP and is exposed to few geographic influences; i.e., there is little coastal upwelling and only limited inputs of terrigenous nutrients (Fig. 1; Sagawa et al., 2012). The main surface current around our study site is the North Equatorial Countercurrent (NECC), which runs between the equator and 10°N in the modern western Pacific (Toole et al., 1988; Lukas et al., 1991). The main sources of the NECC are the Mindanao Current and the reversing South Equatorial Current (SEC; Lukas et al., 1991). The main water masses include the

upper South Pacific Subtropical Water, and below this the water masses are characterized by lower salinities and influenced mainly by the North Pacific Intermediate Water (NPIW) and/or the Antarctic Intermediate Water (AAIW; Zenk et al., 2005).

3. Materials and methods

3.1. Materials

Site U1490 was drilled in 2016 during International Ocean Discovery Program (IODP) Expedition 363 on the northern flank of the Eauripik Rise (5°48.95′N, 142°39.27′E) in a water depth of 2341 m (Fig. 1; Rosenthal et al., 2018). Using the three holes retrieved from Site U1490, a continuous splice was constructed that covers the early Miocene to recent times and has a mean sedimentation rate of approximately 1–2 cm/kyr (Rosenthal et al., 2017). The upper 185 m is composed mainly of foraminifer-rich nannofossil ooze with a small amount of clay (Rosenthal et al., 2018). For this study, 10 cc of sediments were sampled at 20 cm intervals between depths of 38 m and 97 m composite core depth below seafloor (CCSF) from the primary splice (Table 1). These samples span the Pliocene to the early Pleistocene with a mean temporal resolution of around 8–10 kyr.

3.2. Foraminiferal stable carbon and oxygen isotope analysis

The samples were dried in an oven at 60 °C for over 24 h and their dry bulk weight was determined before wet-sieving through a 63 μm sieve using ultrapure water. Then, the coarse components were oven-dried again at 60 °C. The planktonic foraminiferal species *T. sacculifer* without sac-like last chamber, and the species *G. tumida*, were selected as the ideal species for this study (Cléroux et al., 2013; Raddatz et al., 2017; Regenberg et al., 2009; Rippert et al., 2016), since these two species existed throughout the Pliocene (Kennett and Srinivasan, 1983) and are relatively abundant in our sample. In addition, preservation of foraminifera tests in our sample is very good to good (Rosenthal et al., 2018) due to the shallower depth of Site U1490 compared with modern WTP lysocline (~3500 m; Wu and Berger, 1991). *T. sacculifer* calcifies at the bottom of the mixed layer and in the uppermost thermocline (45–95 m; Hollstein et al., 2017). The species *G. tumida* calcifies between water depths of 230 and 265 m in the WTP and is therefore useful for monitoring changes in the bottom of the thermocline structure in our study area (Hollstein et al., 2017). Sediment trap studies from the WTP show that *T. sacculifer* and *G. tumida* can be found throughout the year around our study area (Kawahata et al., 2002; Yamasaki et al., 2008). For stable isotope and other geochemical analysis (e.g., Mg/Ca), 50 tests of *T. sacculifer*, 40 tests of *G. tumida* and 1–4 tests of the benthic species *C. wuellerstorfi* were picked from each sample from the 315–355 μm size fraction. These foraminiferal tests were then gently crushed between two glass plates to open the chambers. All benthic sample fragments and one-third of the planktonic sample fragments were used for stable isotope analysis. The remaining two-thirds of the planktonic fragments were used for other geochemical analysis. All isotope analysis was conducted using a Thermo Fisher Scientific MAT 253 mass spectrometer combined with a Kiel IV carbonate preparation device at GEO-MAR. We calibrated our results against the NBS-19 (National Bureau of Standards) carbonate standard and an in-house standard ("Standard Bremen"). The isotope values are presented in the delta notation ($\delta^{18}O$, $\delta^{13}C$) and reported as ‰ relative to the Vienna Pee Dee Belemnite (VPDB) standard. The long-term
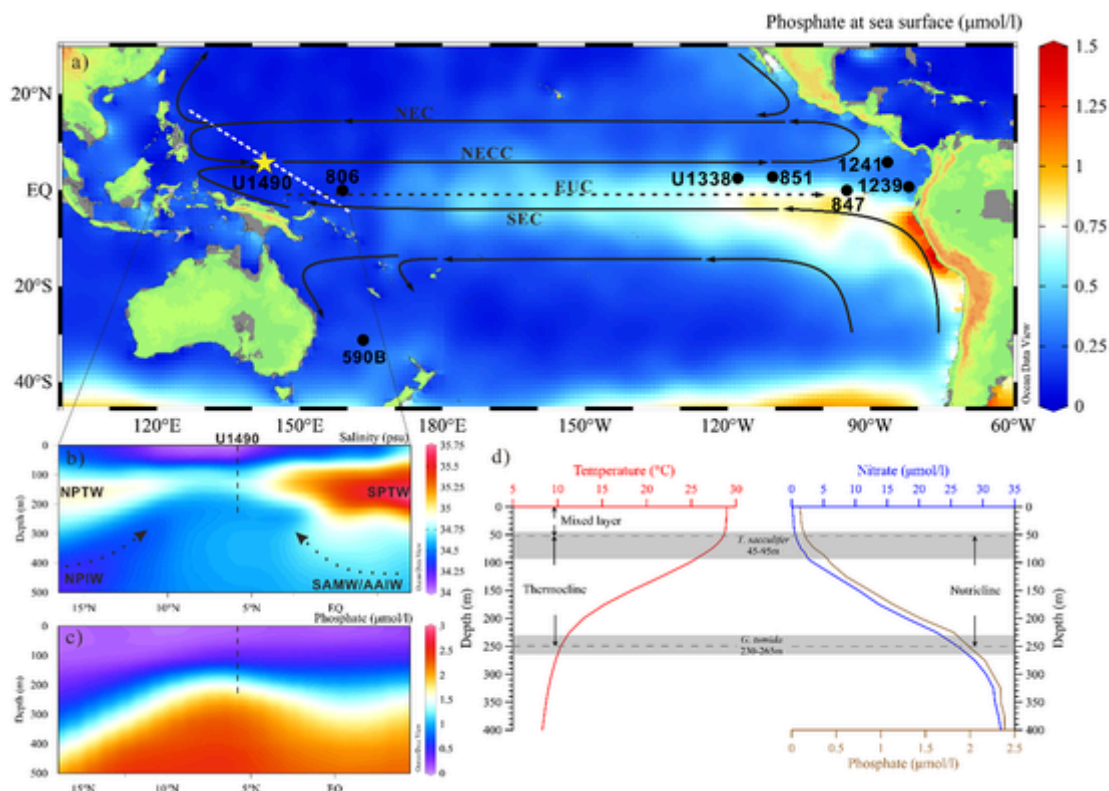
Fig. 1. (a) Colour-coded chart of the equatorial Pacific showing the mean annual sea surface phosphate concentration. The most important tropical Pacific surface currents are indicated. Yellow star = Site U1490; black dots = reference sites. The white dotted line indicates the location of cross sections (b) and (c), which show water mass salinity and phosphate, respectively. (d) Profiles of sea water temperature, phosphate, and nitrate for the upper 400 m of the sea area at Site U1490. NEC = North Equatorial Current; NECC = North Equatorial Counter Current; EUC = Equatorial Undercurrent; SEC = South Equatorial Current; SPTW = South Pacific Tropical Water; NPTW = North Pacific Tropical Water; SAMW = Subantarctic Mode Water; AAIW = Antarctic Intermediate Water; NPIW = North Pacific Intermediate Water. All data from World Ocean Atlas 13 (WOA13; Garcia et al., 2014; Locarnini et al., 2013; Zweng et al., 2013). (For interpretation of the references to colour in this figure legend, the reader is referred to the web version of this article.)

Table 1
Sampling information of IODP Site U1490 in this study.

Top of splice interval					Bottom of splice interval				
Hole	Core	Section	Interval (cm)	Depth CCSF (m)	Hole	Core	Section	Interval (cm)	Depth CCSF (m)
C	5	2	87	37.795	C	5	3	37	38.795
B	5	1	63	38.973	B	5	6	23	46.073
C	6	1	83	46.266	C	6	3	143	49.866
B	6	1	139	50.06	B	6	7	47	58.16
A	7	1	98	58.355	A	7	2	128	60.155
B	7	1	133	60.347	B	7	7	33	68.347
A	8	1	46	68.552	A	8	1	126	69.352
B	8	1	71	69.557	B	8	4	51	73.857
C	10	1	127	74.001	C	10	7	17	81.901
A	9	2	78	82.057	A	9	4	108	85.357
C	11	2	27	85.563	C	11	6	12	91.413
A	10	2	50	91.621	A	10	3	140	94.021
B	11	1	57	94.226	B	11	2	147	96.626

analytical precision was $\pm$ 0.06‰ for $\delta^{18}O$ and $\pm$ 0.05‰ for $\delta^{13}C$.

3.3. Bulk-sediment elemental analysis

The freeze-dried samples were ground to form a 200-mesh powder and then ignited at 600 °C to determine the loss on ignition. About 30–45 mg of each sample was then digested using a mixture of HNO_3 + HF on a hot plate. Subsequently, the eluted samples were diluted with 2% HNO_3 prior to major and trace-element analysis using a Thermo-Fisher IRIS Advantage ICP-OES and a Thermo-Fisher X series ICP-MS, respectively, at the State Key Laboratory of Marine Geology in Tongji University, China. Analytical accuracy was assessed by analysis of the BHVO-2, GSP-2, GSD-9, and W-2a standards, which gave results typically within $\pm$ 3% of the certified values for major elements, and within $\pm$ 10% of the certified values for trace elements. Analytical precision, expressed as the relative standard deviation (RSD), was determined by analysis of several duplicate samples and was typically better than 5% for the major elements, and better than 10% for the trace elements (including the rare earth elements). The bulk-sediment Ba/Ti ratios can be used as an index of productivity, with higher Ba/Ti values indicating periods of enhanced productivity (Murray et al., 2000; Nürnberg et al., 1997; Paytan and Griffith, 2007). This proxy assumes that changes in the delivery of Ba in biogenic material are implicit in the bulk ratio measurement, such that any increase in Ba/Ti through time can be interpreted as reflecting the accumulation of excess Ba, which approximates marine productivity (Murray et al., 2000).

3.4. Age model

The shipboard age model for Site U1490 was constructed using calcareous nannofossil and planktonic foraminifera biostratigraphy data, which was supported by the record of paleomagnetic reversals (Rosenthal et al., 2018). As the paleomagnetic data between 1.1 Ma and 8.8 Ma (i.e., 16–175 m below the seafloor, mbsf) could not be interpreted correctly owing to diagenetic overprinting (Rosenthal et al., 2018), and as most of the biodatums showed poor precision in terms of depth, we additionally tuned the $\delta^{18}O$ record of the epibenthic foraminifera

C. wuellerstorfi to the LR04 global benthic δ18O reference stack (Lisiecki and Raymo, 2005; Fig. 2a). This allowed us to establish the first high-precision Site U1490 chronostratigraphy for the period 5.1–2.6 Ma. The close agreement between the two δ18O records allowed us to assign the section between approximately 37.8 and 96.6 m in the U1490 splice to 5.1–2.6 Ma, which

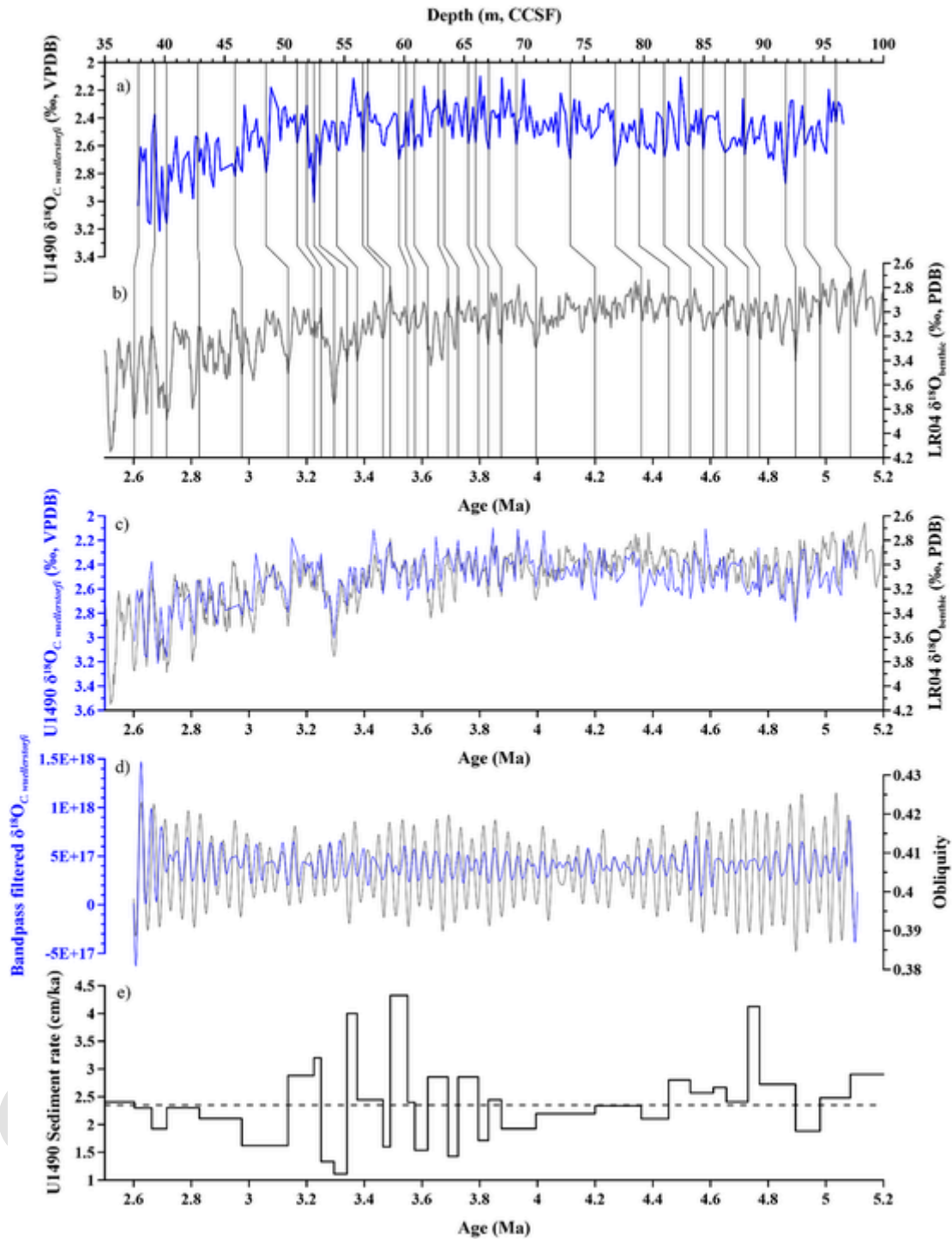equates to an average sedimentation rate of 2–3 cm/kyr (Fig. 2e).

Fig. 2. Site U1490 age model between 5.1 Ma and 2.6 Ma. (a) U1490 benthic δ18O$_{C.wuellerstorfi}$ (blue) versus composite core depth below seafloor (CCSF). (b) LR04 global benthic δ18O reference stack (gray) on age scale (Lisiecki and Raymo, 2005). Vertical lines between (a) and (b) indicate tie-lines between records. (c) U1490 benthic foraminiferal δ18O record (blue) tuned to the LR04 stack (gray). (d) Comparison of 41-kyr band-pass filtered records of U1490 benthic foraminiferal δ18O record and obliquity. The obliquity data are from Laskar et al. (2004). (e) Calculated linear sedimentation rate between 2.6 Ma and 5.1 Ma. The dashed line indicates an average of 2.35 cm/ka. (For interpretation of the references to colour in this figure legend, the reader is referred to the web version of this article.)

4. Results

4.1. Planktonic and benthic foraminiferal $\delta^{13}C$

The $\delta^{13}C_{T.sacculifer}$ and $\delta^{13}C_{G.tumida}$ records from Site U1490 covering the period 5.1–2.6 Ma show high amplitude variations between 1.10‰ and 2.09‰, and between 0.94‰ and 1.80‰, respectively (Fig. 3b, c). Between approximately 5.1 Ma and 4.8 Ma, $\delta^{13}C_{T.sacculifer}$ shows a gradually increasing trend. Between 4.8 Ma and 4.2 Ma, $\delta^{13}C_{T.sacculifer}$ decreases gradually by about 0.5‰, followed by a sharp rise and fall from 4.2 Ma to 3.8 Ma. After a further increase between 3.8 Ma and 3.6 Ma, the $\delta^{13}C_{T.sacculifer}$ record returns to the same level as before 4.8 Ma. The $\delta^{13}C_{G.tumida}$ fluctuations are similar to the $\delta^{13}C_{T.sacculifer}$ record, although the mean value (1.43‰) is lighter than that of *T. sacculifer* (1.6‰; Fig. 3c). In particular, between approximately 4.8 Ma and 4.3 Ma, $\delta^{13}C_{G.tumida}$ increases slightly, while $\delta^{13}C_{T.sacculifer}$ declines. The benthic $\delta^{13}C_{C.wuellerstorfi}$ data range from −0.33‰ to 0.64‰, with an average of 0.19‰. Compared with the planktonic $\delta^{13}C$ profiles, benthic $\delta^{13}C$ generally exhibits similar variations but with significantly different amplitudes (Fig. 3d).

4.2. $\delta^{13}C$ gradients in Site U1490

To explore changes in nutricline depth and productivity in the WTP, we estimated the $\delta^{13}C$ differences between *T. sacculifer* and *G. tumida* (surface-to-thermocline gradient, $\Delta\delta^{13}C_{sac-tum}$) and between *T. sacculifer* and *C. wuellerstorfi* (surface-to-deep gradient, $\Delta\delta^{13}C_{sac-benthic}$) at Site U1490 as indicators of nutricline depth and productivity, respectively (Fig. 4a, b). The $\Delta\delta^{13}C_{sac-tum}$ value is generally higher between 5.1 Ma and 4.8 Ma, then decreases sharply around 4.8 Ma and maintains this relatively lower value between 4.8 Ma and 3.8 Ma, except for a slight

increase at about 4.1 Ma. During the period 3.8–3.5 Ma, $\Delta\delta^{13}C_{sac-tum}$ gradually increases, then maintains relatively higher values between 3.5 Ma and 3.0 Ma, but decreases again between 3.0 Ma and 2.6 Ma. Similarly, the $\Delta\delta^{13}C_{sac-benthic}$ record is characterized by higher or increasing values between 5.1 Ma and 4.8 Ma, then decreases and maintains lower values between 4.8 Ma and 3.8 Ma, except for an increase around 4.1 Ma. Values gradually increase during 3.8–3.5 Ma, then reach higher values between 3.5 Ma and 2.6 Ma. That is, in general, smaller surface-to-thermocline gradients in the carbon isotope records roughly covary with low surface-to-deep gradients in our study area.

4.3. Ba/Ti changes at Site U1490

The Ba/Ti profile from Site U1490 shows prominent and well-defined staged changes over longer timescales. That is, the Ba/Ti ratios are high between 5.1 Ma and 4.8 Ma, then decline rapidly around 4.8 Ma and remain at these lower levels until 3.8 Ma (Fig. 4c). Subsequently, the Ba/Ti ratio gradually increases between 3.8 Ma and 3.5 Ma as a period of transition from long-term higher to lower productivity, and then sustains higher values between 3.5 Ma and 3.0 Ma, before decreasing again from 3.0 Ma to 2.6 Ma.

5. Discussion

5.1. Reconstruction of nutricline depth and productivity based on foraminiferal $\delta^{13}C$

As different planktic foraminiferal species have specific preferred depth habitats, their isotope-geochemical compositions can be used to reconstruct the upper water column structure (e.g., Hollstein et al., 2017; Steinke et al., 2010). Notably, the various species reveal different
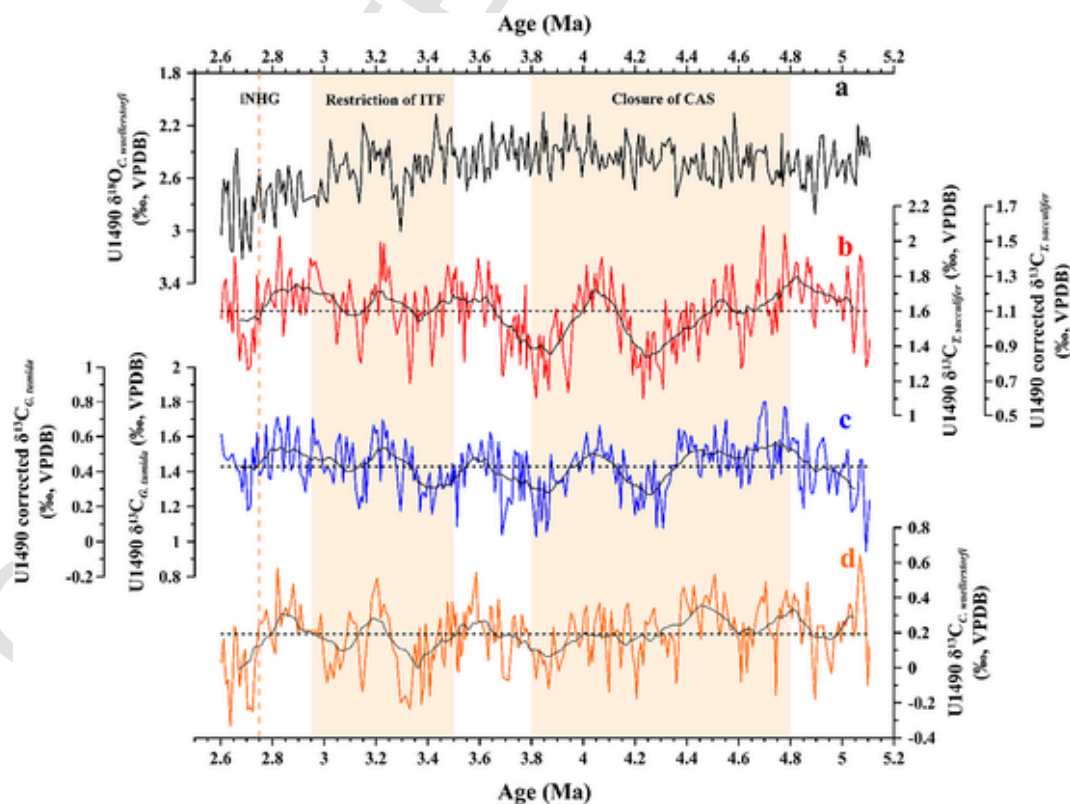
Fig. 3. Pliocene $\delta^{13}C$ records from Site U1490. (a) U1490 benthic $\delta^{18}O_{C.wuellerstorfi}$ on age scale for reference. (b) $\delta^{13}C$ record of surface-dwelling planktonic foraminifer *T. sacculifer*. Extra Y axis represents the corrected $\delta^{13}C$ scale after equilibrium correction. (c) $\delta^{13}C$ record of thermocline-dwelling planktonic foraminifer *G. tumida*. Extra Y axis represents the corrected $\delta^{13}C$ scale after equilibrium correction. (d) $\delta^{13}C$ record of benthic foraminifer *C. wuellerstorfi*. The $\delta^{13}C$ records are shown with their long-term trends (17-running averages). Dashed lines indicate mean values of these records. CAS = Central American Seaway; ITF = Indonesian Throughflow; iNHG = intensification of Northern Hemisphere Glaciation.
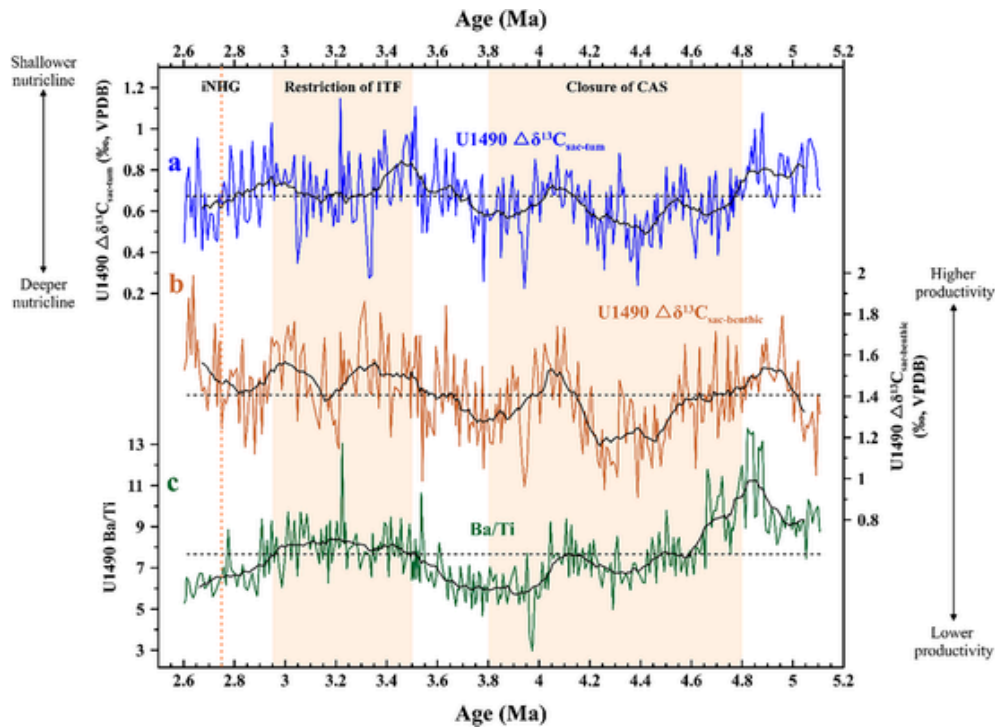
Fig. 4. Evolution of nutricline and productivity at IODP Site U1490. (a) Gradient between *T. sacculifer* and *G. tumida* $\delta^{13}C$ (surface-to-thermocline gradient: $\Delta\delta^{13}C_{sac\text{-}tum}$). (b) Gradient between *T. sacculifer* and *C. wuellerstorfi* $\delta^{13}C$ (surface-to-deep gradient: $\Delta\delta^{13}C_{sac\text{-}benthic}$). (c) Ba/Ti ratios. CAS = Central American Seaway; ITF = Indonesian Throughflow; iNHG = intensification of Northern Hemisphere Glaciation.

$\delta^{13}C$ fractionations between biogenic calcite and dissolved inorganic carbon (DIC) in seawater due to vital effects (Birch et al., 2013; Cannariato and Ravelo, 1997; Ravelo and Fairbanks, 1995; Ravelo et al., 1990; Rippert et al., 2016). According to previous studies, $\delta^{13}C$ values obtained from *T. sacculifer* and *G. tumida* are shifted by −0.5‰ and − 1.0‰, respectively, with respect to the $\delta^{13}C$ changes of DIC in seawater ($\delta^{13}C_{DIC}$; Cannariato and Ravelo, 1997; Ravelo and Fairbanks, 1995). These offsets have been used to correct the long-term planktic foraminifera $\delta^{13}C$ records in order to remove the influence of vital effects (Cannariato and Ravelo, 1997; Reghellin et al., 2020). To better assess the $\delta^{13}C_{DIC}$, the $\delta^{13}C$ records of planktic foraminifera presented here have been corrected for these equilibrium offsets (Fig. 3b, c; Cannariato and Ravelo, 1997; Ravelo and Fairbanks, 1995). $\delta^{13}C_{DIC}$ is predominately controlled by global carbon changes (interactions among atmospheric, terrestrial and oceanic carbon reservoirs) and local shifts created mainly by changes in nutrient supply and utilization (Steph et al., 2006; Tiedemann et al., 2007). Thus, the differences in the corrected carbon isotope compositions of planktic foraminifera that lived in the mixed layer and thermocline have been widely used to reconstruct upper-ocean nutrient structures (e.g., Beltran et al., 2014; Mulitza et al., 1998).

Vertical migration of planktic foraminifera species over their live times might have been crucial of the $\delta^{13}C$-signal formation, and needs to be considered cautiously. Core top analyses indicate that *T. sacculifer* reflects mixed layer conditions in the WTP (Hollstein et al., 2017; Sagawa et al., 2012). Cannariato and Ravelo (1997) have proposed that a general lack of a linear trend between $\delta^{18}O$ and $\delta^{13}C$ values coupled with the overall small range (~1.0‰) implies that *T. sacculifer* calcified in the surface mixed layer during the Pliocene even when considering depth migrations. As our *T. sacculifer* $\delta^{13}C$ values also span a similar small range (~0.99‰) during the Pliocene, we here assume that *T. sacculifer* calcified in the surface mixed layer, where nutrient concentrations are relatively low. Instead, *G. tumida* reflects lower thermocline conditions (Hollstein et al., 2017; Sagawa et al., 2012). Previous studies

indicate that *G. tumida* calcifies close to the bottom of the photic zone, which acts as an anchor point to reflect thermocline changes (Cannariato and Ravelo, 1997; Ravelo and Fairbanks, 1995). In addition, Ford et al. (2015) clarified that the long-term subsurface cooling trend in *G. tumida* was related to alterations in thermocline conditions rather than a change in its depth habitat in the WTP. As the nutricline and thermocline are tightly coupled in the modern WTP (Fig. 1d), we suggest that differences in the $\delta^{13}C$ fluctuations between *T. sacculifer* and *G.tumida* reflect nutricline depth variations.

As phosphate concentrations are usually very low in tropical surface waters (Fig. 1a, c, d), the reduced $\delta^{13}C$ difference between mixed layer and thermocline-dwelling species (e.g. $\Delta\delta^{13}C_{sac\text{-}tum}$) implies correspondingly lower nutrient concentration in the thermocline waters, and thus a deeper nutricline (Mulitza et al., 1998; Beltran et al., 2014). Regarding the past conditions, Pliocene thermocline reconstructions along the equatorial Pacific reveal that the WTP thermocline was deeper during the early Pliocene compared to today (Ford et al., 2015). We therefore assume that the phosphate concentrations in the WTP surface water were also close to zero in the Pliocene due to this deeper thermocline. Thus, $\Delta\delta^{13}C_{sac\text{-}tum}$ from our study site can be used as an indicator of nutricline depth. In terms of physical oceanography, nutricline changes would indicate that an increase in upwelling parallels increased nutrient content in the deep waters (Schmidt et al., 1993). Consequently, the depth of the nutricline reflects nutrient supply to the upper ocean (Cermeño et al., 2008).

Phytoplankton prefers to absorb ^{12}C through photosynthesis, leading to heavier $\delta^{13}C$ in the upper layer. During the decomposition of sinking organic carbon ^{12}C is released into the deeper depth levels, which in turn leads to a lighter $\delta^{13}C$ close to the seafloor (Berger and Vincent, 1986). The differences in $\delta^{13}C$ records between planktonic and benthic foraminifera have been used as a qualitative indicator of productivity in tropical and subtropical oceans, with larger values indicating a period of increased productivity (Sarnthein and Winn, 1990; Jian et al., 2001; Li et al., 2010). Consequently, the differences in $\delta^{13}C$

records between *T. sacculifer* and *C. wuellerstorfi* ($\Delta\delta^{13}C_{sac-benthic}$) from our study site can be used to approximate changes in productivity.

5.2. Coupling of nutricline and productivity variability in the WPWP

Since the low-latitude processes and its dynamics of WTP and ETP are tightly coupled both in the present and past, we first compare Site U1490 $\delta^{13}C$ records to those from ETP sites. The benthic $\delta^{13}C$ records from Ocean Drilling Program (ODP) Site 1241 and other sites in the ETP reflect shifts in the carbon budget of the global ocean (Mix et al., 1995; Steph et al., 2006; Tiedemann et al., 2007). Fig. 5 shows the comparisons between our Site U1490 benthic $\delta^{13}C$ records and the benthic $\delta^{13}C$ records from ETP Site 1241. It is evident that the benthic U1490 $\delta^{13}C$ profile broadly follows the benthic $\delta^{13}C$ record of ETP Site 1241 (Tiedemann et al., 2007; Fig. 5 and Fig. S1). Likewise, long-term fluctuations of our planktonic foraminifera $\delta^{13}C$ records are similar to benthic and planktonic foraminifera $\delta^{13}C$ records from the ETP (ODP Sites 1241 and 851; Cannariato and Ravelo, 1997; Steph et al., 2006). Thus, we suggest that these similar variations in the Site 1490 planktonic foraminifera $\delta^{13}C$ records broadly reflect the global carbon cycle during the Pliocene (Fig. 5 and Fig. S1). Besides, there is an interesting observation that the *T. sacculifer* $\delta^{13}C$ values from ETP Sites 851 and 1241 are obviously higher than those from Site U1490. This phenomenon might have resulted from the overall higher productivity in the ETP than that in the oligotrophic WTP. Higher productivity generally leads to ^{12}C depletion in surface water, remaining heavier $\delta^{13}C$ in DIC as well as foraminiferal calcite (Ravelo and Hillaire-Marcel, 2007). With the biological pump bringing ^{12}C-riched organic carbon into the deep ocean, benthic $\delta^{13}C$ generally becomes lighter due to the respiration/oxidization of such ^{12}C-riched carbon. Consequently, the benthic $\delta^{13}C$ difference between WTP and ETP is opposite to the $\delta^{13}C$ difference in *T. sacculifer*, with higher benthic $\delta^{13}C$ values at Site U1490 and lower values at ETP Site 1241 (Fig. 5). These opposite $\delta^{13}C$ differences also infer a larger surface to benthic $\delta^{13}C$ gradient in the ETP, which further implies that the productivity in the WTP was lower than in the ETP throughout the Pliocene.

Although affected mainly by the Pliocene global carbon cycle (Fig. 5), there are still subtle differences in the $\delta^{13}C$ fluctuations of the two planktonic species from Site U1490 (Fig. 5), which were most probably caused by locally differential nutrient supply and utilization. Therefore, we used the $\delta^{13}C$ differences between the two species (i.e., $\Delta\delta^{13}C_{sac-tum}$) as an indicator of changes in the nutricline depth, excluding the common global carbon cycle signature (see Section 5.1).

Increased $\Delta\delta^{13}C_{sac-tum}$ values point to a shallower nutricline and vice versa (Fig. 6a). During 5.1–4.8 Ma, the generally higher $\Delta\delta^{13}C_{sac-tum}$ value indicates that the nutricline was rather shallow. After ~4.8 Ma, the decreasing $\Delta\delta^{13}C_{sac-tum}$ implies a significant deepening of the nutricline, while the nutricline maintained a relatively deep position between 4.8 Ma and 3.8 Ma, except for a slightly shoaling at ~4.1 Ma. Over the period 3.8–3.5 Ma, the nutricline again started to shoal, and maintained a shallower level until 3.0 Ma before deepening again between 3.0 Ma and 2.6 Ma.

To investigate the temporal changes in marine productivity, we used the $\Delta\delta^{13}C_{sac-benthic}$ and Ba/Ti records from Site U1490 (see Section 5.1). By comparing these with changes in the nutricline depth, we found a good covariant relationship between nutricline depth and productivity changes in our study area (Fig. 6a, b, c, and Fig. S2). The period between 5.1 Ma and 4.8 Ma was characterized by an overall shallower nutricline and increased productivity (Fig. 6a, b, c). Specifically, the Ba/Ti values were significantly higher than those during other periods. Between 4.8 Ma and 3.8 Ma, the nutricline deepened and remained at relatively deeper levels, and the productivity records showed similar decreasing values. During 3.8–3.5 Ma, productivity increased slowly and was accompanied by a gradual shoaling of the nutricline. The period between 3.5 Ma and 3.0 Ma was again characterized by an overall shallower nutricline and increased productivity (Fig. 6a, b, c).
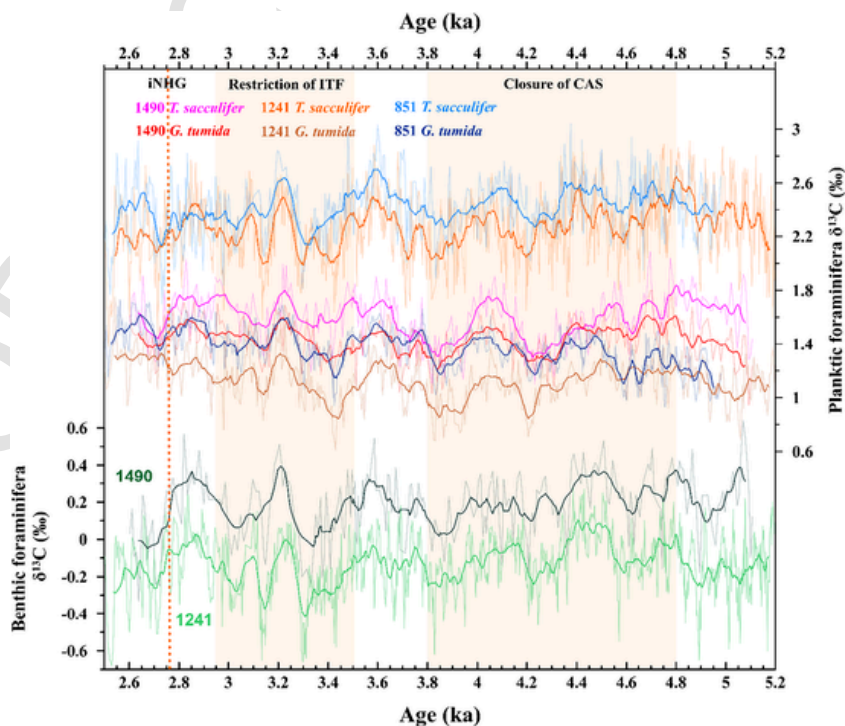

Fig. 5. Comparison of Site U1490 foraminiferal $\delta^{13}C$ records with according records from ETP Sites 851 (Cannariato and Ravelo, 1997) and 1241 (Steph et al., 2006; Tiedemann et al., 2007). All $\delta^{13}C$ records of planktic foraminifera are based on international reference standards according to original references (PDB or VPDB). CAS = Central American Seaway; ITF = Indonesian Throughflow; iNHG = intensification of Northern Hemisphere Glaciation.
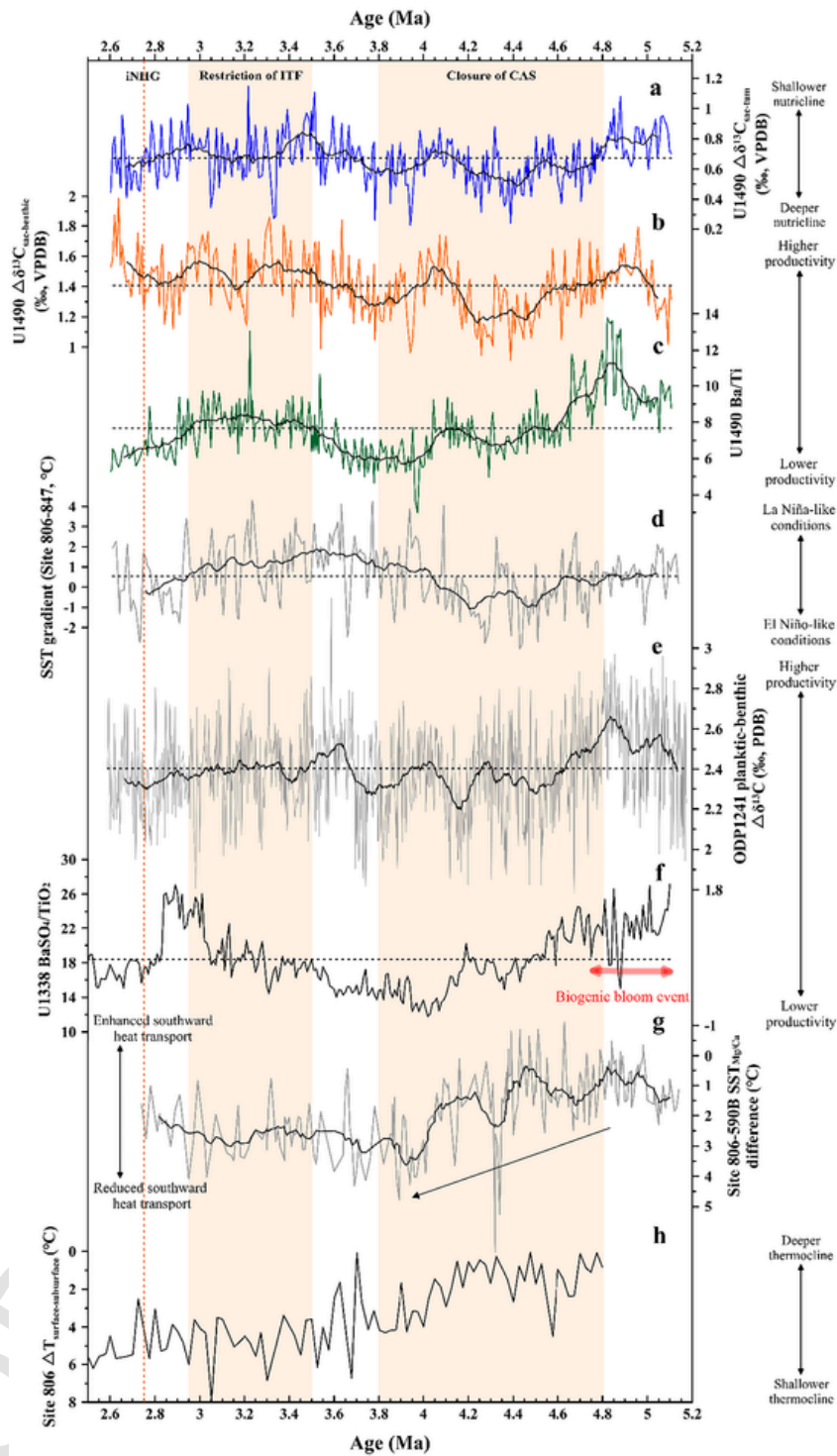
Fig. 6. Proxy data from Site U1490 in relation to other sites. (a) Gradient between U1490 *T. sacculifer* and *G. tumida* $\delta^{13}C$ (surface-to-thermocline gradient: $\Delta\delta^{13}C_{sac\text{-}tum}$) reflecting nutricline variations. (b) Gradient between U1490 *T. sacculifer* and *C. wuellerstorfi* $\delta^{13}C$ (surface-to-deep gradient: $\Delta\delta^{13}C_{sac\text{-}benthic}$) reflecting productivity changes. (c) U1490 Ba/Ti ratios used to approximate productivity changes. (d) SST gradient between ODP Sites 806 and 847 (Wara et al., 2005) as an indicator of past ENSO-like variability. (e) Gradient between planktic and benthic foraminifera $\delta^{13}C$ from Site 1241 (ETP; Steph et al., 2006; Tiedemann et al., 2007). (f) $BaSO_4/TiO_2$ ratios from Site U1338 (ETP; Lyle and Baldauf, 2015). (g) Meridional $SST_{Mg/Ca}$ difference between WPWP Site 806 (Wara et al., 2005) and southwestern Pacific Site 590B (Karas et al., 2011). (h) Vertical $\Delta T_{surface\text{-}subsurface}$ at Site 806 (Ford et al., 2015; Wara et al., 2005). CAS = Central American Seaway; ITF = Indonesian Throughflow; iNHG = intensification of Northern Hemisphere Glaciation.

During 3.0–2.6 Ma, the Ba/Ti ratios indicate that productivity decreased slightly (Fig. 6c). In contrast, the $\Delta\delta^{13}C_{\text{sac-benthic}}$ record points towards a period of greater productivity during 3.0–2.6 Ma, especially after 2.75 Ma (Fig. 6b). The mechanism of such divergence might be that the pre-formed $\delta^{13}C$ value of the subsurface or deep waters changed or the subducting locations of these waters changed with the onset of the NHG. In addition, the atmospheric CO_2 concentration decreased significantly during the iNHG (Willeit et al., 2015), which may have affected the $^{13}C_{\text{DIC}}$ values in the surface waters via air–sea exchange. Hence, $\Delta\delta^{13}C_{\text{sac-benthic}}$ records could be in response to the iNHG, but might not indicate productivity changes as the Ba/Ti ratios showed in this period. In consequence, decreased productivity was accompanied by a deepening of the nutricline in the study area during 3.0–2.6 Ma. Our data suggest that the changes in productivity vary consistently with changes in nutricline depth, which might have been a response to increased nutrient supply. Consequently, we hypothesize that the dynamics of nutricline depth play an important role in regulating productivity, because a shallower nutricline allows increased nutrient supply to the upper ocean, and hence, would foster productivity.

5.3. Response to the early Pliocene "biogenic bloom" and closure of the Central American Seaway

Potential factors, which might have had major impact on the Pliocene WTP productivity and nutricline depth include changes in global carbon cycles, fluctuations in tropical mean state, remote forcing from the Pacific Meridional Overturning Circulation (PMOC) and tectonic events (Burls et al., 2017; Cane and Molnar, 2001; Grant and Dickens, 2002; Nathan and Leckie, 2009; Wells et al., 1999). Published corresponding records from WTP (ODP Site 806), ETP (ODP Sites 847, 1239, 1241 and IODP Site U1338), North Pacific (ODP Site 882) and southwestern Pacific (Deep Sea Drilling Program Site 590B) are involved in this study to evaluate and figure out the possible mechanisms of the long-term variations in productivity and nutricline depth. According to Farrell et al. (1995) and Lyle and Baldauf (2015), a "biogenic bloom event" occurred between approximately 6.7 Ma and 4.5 Ma in the ETP, which was characterized by an overall increase in biogenic accumulation along the equator. This event has been observed primarily in the tropical Indo-Pacific (Farrell et al., 1995), but also in other parts of the global ocean. Intense biogenic blooms have been also reported from the sediment cores in the Indian Ocean between 6.0 Ma and 5.0 Ma (Dickens and Owen, 1999; Imai et al., 2020), and in the Atlantic Ocean at 8.2–5.4 Ma, 6.6–6.0 Ma, and at ~5.0 Ma (Diester-Haass et al., 2005). Therefore, biogenic bloom events can be regarded as global phenomena, although the timing of their occurrence might have been variable and the trigger mechanisms still remain unknown (Imai et al., 2020). As shown in Figs. 6a, b and c, a stable shallower nutricline and higher productivity during 5.1–4.8 Ma were also observed in our records. For that reason, we suggest that the stable shallow nutricline and increased productivity conditions over the period 5.1–4.8 Ma appear to be a regional response of the global biogenic bloom event.

Modern ENSO events typically associated with variations of the trade winds and the Walker Circulation (Etourneau et al., 2010) commonly result in a seesaw productivity anomaly across the tropical Pacific. Turk et al. (2001) found that a shallower nutricline and greater productivity in the WPWP likely develop during modern El Niño conditions, when the WPWP thermocline is relatively shallow, while in the ETP a deeper nutricline leads to reduced marine productivity. We use this framework to investigate changes in mean nutricline and productivity states during the Pliocene, although the dynamics of the tropical Pacific mean state changes on tectonic timescales are not the same as modern climate dynamics, which generate interannual El Niño events (Fedorov et al., 2013). Here we use the Pliocene tropical Pacific west–east sea surface temperature (SST) gradient (Fig. 6d), which is based on Mg/Ca$_{T\ sacculifer}$-derived Pliocene SST records from ODP Sites

806 and 847 (Wara et al., 2005), as an indicator of how El Niño-like or La Niña-like conditions changed in the past, and compared our nutricline and productivity changes to this gradient. At ~4.8 Ma, a remarkable turning point (Fig. 6a, b, c) is followed by a period with a relatively deep nutricline and low productivity (i.e., oligotrophic conditions; 4.8–3.5 Ma). Similarly, productivity was low in the ETP, where low biogenic opal accumulation rates (at ODP Site 1239) point to low diatom productivity between 4.8 Ma and 3.8 Ma (Steph et al., 2010). In addition, the comparison of our productivity records (Fig. 6b, c) with corresponding records from ETP Sites 1241 and U1338 (Lyle et al., 2019; Steph et al., 2006; Fig. 6e, f), shows no inverse relationship of productivity between the WTP and ETP. We therefore conclude that variations in the trade winds combined with corresponding Walker Circulation changes or west–east seesaw fluctuations of tropical mean state can be ruled out as primary drivers of early Pliocene changes in biogenic production and nutricline depth. Bolton et al. (2010) support this interpretation as they also found no evidence of productivity control by either west–east tilting or basin-wide diabatic movements of the thermocline in the late Pliocene tropical Pacific.

Alternatively, the northern-sourced water masses formed at high-latitudes might have contributed to the tropical Pacific nutrient inventory, and hence, marine productivity (Haug et al., 1999). One key process in this respect is the evolution of the PMOC, because the strengthened inter-basin gradient and thus enhanced PMOC can increase the supply rate of silicates to the subarctic Pacific surface through vertical exchange and upwelling, leading to increased productivity in the subarctic Pacific (Burls et al., 2017; Haug et al., 1999). Consequently, upwelling in the subarctic Pacific represents a potential route for high-nutrient deeper waters to get entrained into intermediate and surface-water, thus affecting the nutrient conditions in the low-latitudes (Burls et al., 2017; Haug et al., 1999). Hence, the development of the PMOC may be a functional alternative to explain the productivity variations in the low-latitude regions and at the southern margin of the subarctic North Pacific during the Pliocene.

Unfortunately, we found no covariant relationship between productivity changes (i.e. Ba/Ti) in our study area and opal accumulation rates from ODP Site 882 in the subarctic North Pacific. Even when combined with productivity changes from Sites U1490 and 882 by cross-correlation analysis, no obvious positive correlation was found (Fig. S2). The missing correlation might indicate that northern Pacific-sourced nutrient-rich water masses were not responsible for nutricline and productivity changes in our study area. In addition to nutrient supply from the North Pacific, changes of sea water pH might have affected productivity in the tropical Pacific. According to Shankle et al. (2021), the higher productivity in the ETP can be explained by i) more acidic water than modern ETP and ii) decoupled zonal pH and temperature gradients across the tropical Pacific in response to a strengthened PMOC during the Pliocene. However, as there is no significant difference in pH between modern and Pliocene (Shankle et al., 2021), and as the pH changes in the Pliocene WTP were likely too small to effectively cause productivity changes, we speculate that the productivity changes in our study area must have been caused by other processes. Further, the missing correlation to Site 882 might be due to the fact that Site 882 is too far in the north, located north of the highly variable Kuroshio/Oyashio system in the subarctic North Pacific (Masujima et al., 2003; Nakano et al., 2018).

At ~4.8 Ma, the closing of the Central American Seaway reached a critical point (Haug et al., 2001; Haug and Tiedemann, 1998; Steph et al., 2006), initiating circulation changes (Schneider and Schmittner, 2006) and large-scale oceanic nutrient redistribution. In particular, the distinct and permanent shift in the tropical Pacific maximum opal mass accumulation rate at ~4.4 Ma was causally linked to the final closure of the CAS (Farrell et al., 1995), supported by model simulations

(Schneider and Schmittner, 2006). During 4.6–4.0 Ma, the observed surface cooling/freshening at Deep Sea Drilling Program (DSDP) Site 590B shows the meridional SST gradient between the WPWP and the southwestern Pacific (Tasman Sea) increased continuously, indicating weakened East Australian Current (EAC) and surface heat transport towards the southwestern Pacific, which presumably related to the closure of the CAS (Fig. 6g; Karas et al., 2011). Although the reliability of Mg/Ca-derived temperature records of Site 590B were questioned since the changes in water pH caused by a decline in upwelling of old waters might significantly affect planktonic foraminifera Mg/Ca (Dickens and Backman, 2012). Karas et al. (2012) provided the *T. sacculifer* δ^{13}C records of Site 590B, suggesting that their study area did not experience a distinct decline in deep and cold upwelling during the Pliocene. Therefore, we would like to take the Mg/Ca-derived temperature difference between Sites 806 and 590B as an available proxy of meridional SST gradient.

Evidenced by the increased meridional SST gradient (Fig. 6g), the reduced southward heat transport has been interpreted as a response to the closure of the CAS (Karas et al., 2011), with the effect that the oceanic heat retained in the tropical Pacific. Chaisson and Ravelo (2000) have suggested that after 4.5 Ma the vertical subsurface temperature in the WTP remained relatively warm, pointing to a thick mixed layer. This notion is also supported by the surface-to-subsurface vertical temperature gradient ($\Delta T_{surface-subsurface}$) at central WPWP, which implies a deeper thermocline during the period ~4.8–4.0 Ma (Ford et al., 2015; Fig. 6h) and thus an expanded mixed layer. In the WPWP, consequently, a thick mixed layer developed, and nutrient-rich intermediate waters were located beyond the reach of Ekman pumping, so that only nutrient-poor mixed-layer water masses were brought to the surface (Berger et al., 1993; Chaisson and Ravelo, 2000). We therefore speculate that between 4.8 Ma and 3.8 Ma, the general low levels of productivity might have been the result of a thick mixed layer and thus a deeper nutricline, which acted as a barrier to the vertical transport of nutrients responding to the closure of CAS.

5.4. Response to the restriction of the Indonesian Seaway

During ~3.5–3.0 Ma, the west–east SST gradient (Wara et al., 2005) points to predominantly La Niña-like conditions, although the highly variable SST gradient implies a rather unstable mean state across the tropical Pacific (Fig. 6d). Over this same period, however, an overall shallower nutricline and increased productivity developed at our WPWP study site (Fig. 6a, b, c), which is contradictory to La Niña-like conditions. Also in the ETP (Sites 1241 and U1338), both the $\Delta\delta^{13}C_{planktic-benthic}$ and $BaSO_4/TiO_2$ ratios point to an overall shallower nutricline and increased productivity, indicated by slightly higher or equal values than over the period 4.8–3.5 Ma, and especially between 4.6 Ma and 3.5 Ma, with no values that are significantly lower than in the WTP (Lyle and Baldauf, 2015; Steph et al., 2006). We therefore suggest that during the period 3.5–3.0 Ma the west–east tropical fluctuations between La Niña-like and El Niño-like climate states were most likely not driving marine productivity changes in our study area.

Rather, the high-latitude sourced intermediate waters (specifically, the Subantarctic Mode Water, SAMW) are delivering nutrients to the equatorial Pacific thermocline (Palter et al., 2010; Sarmiento et al., 2004; Toggweiler et al., 1991). During 3.5–3.0 Ma, Karas et al. (2011) interpreted the significant freshening and cooling subsurface water at Tasman Sea Site 590B in terms of the increasing presence of the southern-sourced SAMW/AAIW, in line with the gradual establishment of the Antarctic Frontal System (Fig. S3). As the main conduit of nutrients from the Southern Ocean to the equatorial Pacific, the SAMW/AAIW was similarly allowed to migrate northwards and ventilate via "ocean

tunnelling" into the Subtropical Gyre, and then affect the thermocline in the tropical Pacific (Bostock et al., 2010; Sarmiento et al., 2004). Higher $\Delta T_{surface-subsurface}$ at Site 806 throughout the period 3.5–3.0 Ma also points to a continuous shoaling thermocline (Ford et al., 2015; Fig. 6h) and nutricline (Fig. 6a) in the WTP, which was likely attributed to the invasion of cooler and eutrophic SAMW/AAIW. At the same time, the ongoing constriction of the ITF (Karas et al., 2009; Karas et al., 2017) prevented a large proportion of the southern-Pacific-sourced water from flowing through the Indonesian Seaway into the tropical Indian Ocean, and more southern-sourced water might have remained in the WTP instead (Auer et al., 2019; Cane and Molnar, 2001). Thus, the northward migration of the SAMW/AAIW between 3.5 Ma and 3.0 Ma implies that the higher productivity at WTP Site U1490 might have been influenced by the cooler and nutrient-enriched SAMW/AAIW via "ocean tunnelling". Karas et al. (2011) suspected that the continuous restriction of the Indonesian Seaway contributed, via the cooling of the southern Indian and Atlantic oceans, to the development of the present Antarctic Frontal System, with stronger westerly winds leading to cooling and/or northward migration of the Mode Waters. In consequence, changes in nutricline and productivity at Site U1490 might have additionally responded to the constriction of the ITF.

During 3.0–2.6 Ma, and especially after ~2.75 Ma, the nutricline deepened slightly in our study area, and the Ba/Ti ratios decreased slightly indicating lower productivity. The change in subsurface flow through the ITF from the South Pacific to the North Pacific was complete after ~2.95 Ma (Karas et al., 2009). The decreasing productivity in the WTP during the intensification of the Northern Hemisphere glaciation (< 2.75 Ma) might have been caused by the weakened influence of a cooler and nutrient enriched SAMW.

6. Conclusions

In this study, we used foraminifera carbon isotope and geochemical records obtained from IODP Site U1490, which is located within the NECC in the central WPWP, to provide new insights into Pliocene nutricline dynamics and changes in marine productivity between 5.1 Ma and 2.6 Ma. We also discussed the WPWP nutricline and productivity changes in relation to tectonically related oceanic reorganizations in the CAS and ITF. Our main conclusions are as follows.

(1) The records of temporal change in the nutricline and productivity levels show synchronous long-term variations; i.e., coupled variations between the nutricline and productivity in our study area over tectonic timescales. The dynamics of the nutricline play an important role in regulating productivity in the WTP.

(2) Between 4.8 Ma and 3.5 Ma, the general deepening of the nutricline was accompanied by a decline in productivity. This might have been fostered by the closure of the CAS, leading to the thickening of the mixed layer and the deepening of the nutricline in the WPWP, which acted as a barrier to the vertical transport of nutrients.

(3) The period between 3.5 Ma and 3.0 Ma was characterized by an overall shallower nutricline and increased productivity in our study area, which may have been the result of the restriction of the ITF via the enhanced influence of high-latitude southern-sourced mode waters.

Declaration of Competing Interest

The authors declare that they have no known competing financial interests or personal relationships that could have appeared to influence the work reported in this paper.

Acknowledgements

Appendix A. Supplementary material

Supplementary material to this article can be found online at https://doi.org/10.1016/j.gloplacha.2022.103810.

References

Auer, G., De Vleeschouwer, D., Smith, R.A., Bogus, K., Groeneveld, J., Grunert, P., Castañeda, I.S., Petrick, B., Christensen, B., Fulthorpe, C., Gallagher, S.J., Henderiks, J., 2019. Timing and pacing of Indonesian Throughflow restriction and its connection to late Pliocene climate shifts. Paleoceanogr. Paleoclimatol. 34 (4), 635–657. https://doi.org/10.1029/2018PA003512.

Bali, H., Gupta, A.K., Mohan, K., Thirumalai, K., Tiwari, S.K., Panigrahi, M.K., 2020. Evolution of the oligotrophic West Pacific warm Pool during the Pliocene-Pleistocene boundary. Paleoceanogr. Paleoclimatol. 35 (11). https://doi.org/10.1029/2020PA003875.

Beltran, C., Rousselle, G., Backman, J., Wade, B.S., Sicre, M.A., 2014. Paleoenvironmental conditions for the development of calcareous nannofossil acme during the late Miocene in the eastern equatorial Pacific. Paleoceanography 29 (3), 210–222. https://doi.org/10.1002/2013PA002506.

Berger, W., Vincent, E., 1986. Deep-sea carbonates: reading the carbon-isotope signal. Geol. Rundsch. 75 (1), 249–269. https://doi.org/10.1007/BF01770192.

Berger, W.H., Leckie, R.M., Janecek, T.R., Stax, R., Takayama, T., 1993. Neogene carbonate sedimentation on Ontong Java Plateau: highlights and open questions. In: Berger, W.H., Kroenke, L.W., Mayer, L.A., et al. (Eds.), Proceedings of the Ocean Drilling Program, Scientific Results, 130. Ocean Drilling Program, College Station, TX, pp. 711–744. https://doi.org/10.2973/odp.proc.sr.130.051.1993.

Birch, H., Coxall, H.K., Pearson, P.N., Kroon, D., O'Regan, M., 2013. Planktonic foraminifera stable isotopes and water column structure: Disentangling ecological signals. Mar. Micropaleontol. 101, 127–145. https://doi.org/10.1016/j.marmicro.2013.02.002.

Bolton, C.T., Gibbs, S.J., Wilson, P.A., 2010. Evolution of nutricline dynamics in the equatorial Pacific during the late Pliocene. Paleoceanography 25 (1). https://doi.org/10.1029/2009PA001821.

Bostock, H.C., Opdyke, B.N., Williams, M.J., 2010. Characterising the intermediate depth waters of the Pacific Ocean using $\delta^{13}C$ and other geochemical tracers. Deep-Sea Res. I Oceanogr. Res. Pap. 57 (7), 847–859. https://doi.org/10.1016/j.dsr.2010.04.005.

Brierley, C.M., Fedorov, A.V., Liu, Z., Herbert, T.D., Lawrence, K.T., LaRiviere, J.P., 2009. Greatly expanded tropical warm pool and weakened Hadley circulation in the early Pliocene. Science 323 (5922), 1714–1718. https://doi.org/10.1126/science.1167625.

Brierley, C., Burls, N., Ravelo, C., Fedorov, A., 2015. Pliocene warmth and gradients. Nat. Geosci. 8 (6), 419–420. https://doi.org/10.1038/ngeo2444.

Burls, N.J., Fedorov, A.V., Sigman, D.M., Jaccard, S.L., Tiedemann, R., Haug, G.H., 2017. Active Pacific meridional overturning circulation (PMOC) during the warm Pliocene. Sci. Adv. 3 (9), e1700156. https://doi.org/10.1126/sciadv.1700156.

Cane, M.A., Molnar, P., 2001. Closing of the Indonesian seaway as a precursor to east African aridification around 3–4 million years ago. Nature 411 (6834), 157–162. https://doi.org/10.1038/35075500.

Cannariato, K.G., Ravelo, A.C., 1997. Pliocene–Pleistocene evolution of eastern tropical Pacific surface water circulation and thermocline depth. Paleoceanography 12 (6), 805–820. https://doi.org/10.1029/97PA02514.

Cermeño, P., Dutkiewicz, S., Harris, R.P., Follows, M., Schofield, O., Falkowski, P.G., 2008. The role of nutricline depth in regulating the ocean carbon cycle. Proc. Natl. Acad. Sci. 105 (51), 20344–20349. https://doi.org/10.1073/pnas.0811302106.

Chaisson, W.P., Ravelo, A.C., 2000. Pliocene development of the east–west hydrographic gradient in the equatorial Pacific. Paleoceanography 15 (5), 497–505. https://doi.org/10.1029/1999PA000442.

Cléroux, C., deMenocal, P., Arbuszewski, J., Linsley, B., 2013. Reconstructing the upper water column thermal structure in the Atlantic Ocean. Paleoceanography 28 (3),

503–516. https://doi.org/10.1002/palo.20050.

Dickens, G.R., Backman, J., 2012. A comment on "Pliocene climate change of the Southwest Pacific and the impact of ocean gateways" by C. Karas, D. Nürnberg, R. Tiedemann, D. Garbe Schönberg, EPSL 301, 117–124 (2011). Earth Planet. Sci. Lett. 331–332, 364–365. https://doi.org/10.1016/j.epsl.2011.07.030.

Dickens, G.R., Owen, R.M., 1999. The latest Miocene–early Pliocene biogenic bloom: a revised Indian Ocean perspective. Mar. Geol. 161 (1), 75–91. https://doi.org/10.1016/S0025-3227(99)00057-2.

Diester-Haass, L., Billups, K., Emeis, K.C., 2005. In search of the late Miocene–early Pliocene "biogenic bloom" in the Atlantic Ocean (Ocean Drilling Program Sites 982, 925, and 1088). Paleoceanography 20 (4). https://doi.org/10.1029/2005PA001139.

Driscoll, N., Haug, G., 1998. A short circuit in thermohaline circulation: a cause for northern hemisphere glaciation? Science 282 (5388), 436–438. https://doi.org/10.1126/science.282.5388.436.

Drury, A.J., Lee, G.P., Gray, W.R., Lyle, M., Westerhold, T., Shevenell, A.E., John, C.M., 2018. Deciphering the state of the late Miocene to early Pliocene equatorial Pacific. Paleoceanogr. Paleoclimatol. 33 (3), 246–263. https://doi.org/10.1002/2017PA003245.

Etourneau, J., Schneider, R., Blanz, T., Martinez, P., 2010. Intensification of the Walker and Hadley atmospheric circulations during the Pliocene–Pleistocene climate transition. Earth Planet. Sci. Lett. 297 (1–2), 103–110. https://doi.org/10.1016/j.epsl.2010.06.010.

Farrell, J.W., Raffi, I., Janecek, T.C., Murray, D.W., Levitan, M., Dadey, K.A., Emeis, K.-C., Lyle, M., Flores, J.-A., Hovan, S., Pisias, N.G., Mayer, L.A., Janecek, T.R., Palmer-Julson, A., van Andel, T.H., 1995. Late Neogene sedimentation patterns in the eastern equatorial Pacific Ocean. In: Proceedings of the Ocean Drilling Program, Scientific Results, 138. Ocean Drilling Program, College Station, TX, pp. 717–756. https://doi.org/10.2973/odp.proc.sr.138.143.1995.

Fedorov, A.V., Philander, S.G., 2000. Is El Niño changing? Science 288 (5473), 1997–2002. https://doi.org/10.1126/science.288.5473.1997.

Fedorov, A.V., Dekens, P.S., McCarthy, M., Ravelo, A.C., DeMenocal, P.B., Barreiro, M., Pacanowski, R.C., Philander, S.G., 2006. The Pliocene paradox (mechanisms for a permanent El Niño). Science 312 (5779), 1485–1489. https://doi.org/10.1126/science.1122666.

Fedorov, A.V., Brierley, C.M., Emanuel, K., 2010. Tropical cyclones and permanent El Niño in the early Pliocene epoch. Nature 463 (7284), 1066–1070. https://doi.org/10.1038/nature08831.

Fedorov, A.V., Brierley, C.M., Lawrence, K.T., Liu, Z., Dekens, P.S., Ravelo, A.C., 2013. Patterns and mechanisms of early Pliocene warmth. Nature 496 (7443), 43–49. https://doi.org/10.1038/nature12003.

Ford, H.L., Ravelo, A.C., 2019. Estimates of Pliocene tropical Pacific temperature sensitivity to radiative greenhouse gas forcing. Paleoceanogr. Paleoclimatol. 34 (1), 2–15. https://doi.org/10.1029/2018PA003461.

Ford, H.L., Ravelo, A.C., Hovan, S., 2012. A deep Eastern Equatorial Pacific thermocline during the early Pliocene warm period. Earth Planet. Sci. Lett. 355, 152–161. https://doi.org/10.1016/j.epsl.2012.08.027.

Ford, H.L., Ravelo, A.C., Dekens, P.S., LaRiviere, J.P., Wara, M.W., 2015. The evolution of the equatorial thermocline and the early Pliocene El Padre mean state. Geophys. Res. Lett. 42 (12), 4878–4887. https://doi.org/10.1002/2015GL064215.

Garcia, H.E., Locarnini, R.A., Boyer, T.P., Antonov, J.I., Baranova, O.K., Zweng, M.M., Reagan, J.R., Johnson, D.R., 2014. World Ocean Atlas 2013, Vol. 4: Dissolved Inorganic Nutrients (phosphate, nitrate, silicate). In: Levitus, S. (Ed.), Mishonov, A. Technical Ed.; NOAA Atlas NESDIS 76, 25. https://doi.org/10.7289/V5J67DWD.

Grant, K.M., Dickens, G.R., 2002. Coupled productivity and carbon isotope records in the Southwest Pacific Ocean during the late Miocene–early Pliocene biogenic bloom. Palaeogeogr. Palaeoclimatol. Palaeoecol. 187 (1–2), 61–82. https://doi.org/10.1016/S0031-0182(02)00508-4.

Haug, G.H., Tiedemann, R., 1998. Effect of the formation of the Isthmus of Panama on Atlantic Ocean thermohaline circulation. Nature 393 (6686), 673. https://doi.org/10.1038/31447.

Haug, G.H., Sigman, D.M., Tiedemann, R., Pedersen, T.F., Sarnthein, M., 1999. Onset of permanent stratification in the subarctic Pacific Ocean. Nature 401 (6755), 779–782. https://doi.org/10.1038/44550.

Haug, G.H., Tiedemann, R., Zahn, R., Ravelo, A.C., 2001. Role of Panama uplift on oceanic freshwater balance. Geology 29 (3), 207–210. https://doi.org/10.1130/0091-7613(2001)029<0207:ROPUOO>2.0.CO;2.

Hoerling, M.P., Hurrell, J.W., Xu, T., 2001. Tropical origins for recent North Atlantic climate change. Science 292 (5514), 90–92. https://doi.org/10.1126/science.1058582.

Hollstein, M., Mohtadi, M., Rosenthal, Y., Moffa Sanchez, P., Oppo, D., Martínez Méndez, G., Steinke, S., Hebbeln, D., 2017. Stable oxygen isotopes and Mg/ca in planktic foraminifera from modern surface sediments of the Western Pacific warm Pool: Implications for thermocline reconstructions. Paleoceanography 32 (11), 1174–1194. https://doi.org/10.1002/2017PA003122.

Imai, R., Sato, T., Chiyonobu, S., Iryu, Y., 2020. Reconstruction of Miocene to Pleistocene Sea-surface conditions in the eastern Indian Ocean on the basis of calcareous nannofossil assemblages from ODP Hole 757B. Island Arc 29 (1), e12373. https://doi.org/10.1111/iar.12373.

Jian, Z., Huang, B., Kuhnt, W., Lin, H.-L., 2001. Late Quaternary upwelling intensity and East Asian monsoon forcing in the South China Sea. Quat. Res. 55 (3), 363–370. https://doi.org/10.1006/qres.2001.2231.

Kamikuri, S., Motoyama, I., Nishi, H., Iwai, M., 2009. Evolution of Eastern Pacific warm Pool and upwelling processes since the middle Miocene based on analysis of radiolarian assemblages: Response to Indonesian and central American Seaways. Palaeogeogr. Palaeoclimatol. Palaeoecol. 280 (3–4), 469–479. https://doi.org/10.1016/j.palaeo.2009.06.034.

Karas, C., Nürnberg, D., Gupta, A.K., Tiedemann, R., Mohan, K., Bickert, T., 2009. Mid-Pliocene climate change amplified by a switch in Indonesian subsurface throughflow. Nat. Geosci. 2 (6), 434–438. https://doi.org/10.1038/ngeo520.

Karas, C., Nürnberg, D., Tiedemann, R., Garbe-Schönberg, D., 2011. Pliocene climate change of the Southwest Pacific and the impact of ocean gateways. Earth Planet. Sci. Lett. 301 (1–2), 117–124. https://doi.org/10.1016/j.epsl.2010.10.028.

Karas, C., Nürnberg, D., Tiedemann, R., 2012. The Southwest Pacific during the Pliocene: a reply to Dickens and Backman, 2011. Earth Planet. Sci. Lett. 331–332, 360–363. https://doi.org/10.1016/j.epsl.2012.03.006.

Karas, C., Nürnberg, D., Bahr, A., Groeneveld, J., Herrle, J.O., Tiedemann, R., deMenocal, P.B., 2017. Pliocene oceanic seaways and global climate. Sci. Rep. 7, 39842. https://doi.org/10.1038/srep39842.

Kawahata, H., Nishimura, A., Gagan, M.K., 2002. Seasonal change in foraminiferal production in the western equatorial Pacific warm pool: evidence from sediment trap experiments. Deep-Sea Res. II Top. Stud. Oceanogr. 49 (13–14), 2783–2800. https://doi.org/10.1016/S0967-0645(02)00058-9.

Kennett, J.P., Srinivasan, M.S., 1983. Neogene Planktonic Foraminifera: A Phylogenetic Atlas. Hutchinson Ross Publishing Company, Stroudsberg, Pennsylvania.

Li, T., Zhao, J., Sun, R., Chang, F., Sun, H., 2010. The variation of upper ocean structure and paleoproductivity in the Kuroshio source region during the last 200 kyr. Mar. Micropaleontol. 75 (1–4), 50–61. https://doi.org/10.1016/j.marmicro.2010.02.005.

Laskar, J., Robutel, P., Gastineau, M., Correia, A.C.M., Levrard, B., 2004. A long-term numerical solution for the insolation quantities of the Earth. Astronomy & Astrophysics 428 (1), 261–285. https://doi.org/10.1051/0004-6361:20041335.

Li, L., Li, Q., Tian, J., Wang, P., Wang, H., Liu, Z., 2011. A 4-Ma record of thermal evolution in the tropical western Pacific and its implications on climate change. Earth Planet. Sci. Lett. 309 (1–2), 10–20. https://doi.org/10.1016/j.epsl.2011.04.016.

Lisiecki, L.E., Raymo, M.E., 2005. A Pliocene–Pleistocene stack of 57 globally distributed benthic δ18O records. Paleoceanography 20 (1). https://doi.org/10.1029/2004PA001071.

Locarnini, R.A., Mishonov, A.V., Antonov, J.I., Boyer, T.P., Garcia, H.E., Baranova, O.K., Zweng, M.M., Paver, C.R., Reagan, J.R., Johnson, D.R., Hamilton, M., Seidov, D., 2013. World Ocean Atlas 2013, Vol. 1: Temperature. Levitus, S., Ed., Mishonov A., Technical Ed.; NOAA Atlas NESDIS 73. p. 40. https://doi.org/10.7289/V55X26VD.

Lukas, R., Firing, E., Hacker, P., Richardson, P.L., Collins, C.A., Fine, R., Gammon, R., 1991. Observations of the Mindanao current during the western equatorial Pacific Ocean circulation study. J. Geophys. Res. Oceans 96 (C4), 7089–7104. https://doi.org/10.1029/91JC00062.

Lukas, R., Yamagata, T., McCreary, J.P., 1996. Pacific low-latitude western boundary currents and the Indonesian throughflow. J. Geophys. Res. Oceans 101 (C5), 12209–12216. https://doi.org/10.1029/96JC01204.

Lyle, M., Baldauf, J., 2015. Biogenic sediment regimes in the Neogene equatorial Pacific, IODP Site U1338: Burial, production, and diatom community. Palaeogeogr. Palaeoclimatol. Palaeoecol. 433, 106–128. https://doi.org/10.1016/j.palaeo.2015.04.001.

Lyle, M., Drury, A.J., Tian, J., Wilkens, R., Westerhold, T., 2019. Late Miocene to Holocene high-resolution eastern equatorial Pacific carbonate records: stratigraphy linked by dissolution and paleoproductivity. Clim. Past 15 (5), 1715–1739. https://doi.org/10.5194/cp-15-1715-2019.

Masujima, M., Yasuda, I., Hiroe, Y., Watanabe, T., 2003. Transport of Oyashio water across the subarctic front into the mixed water region and formation of NPIW. J. Oceanogr. 59 (6), 855–869. https://doi.org/10.1023/B:JOCE.0000009576.09079.f5.

McPhaden, M.J., Zebiak, S.E., Glantz, M.H., 2006. ENSO as an integrating concept in earth science. Science 314 (5806), 1740–1745. https://doi.org/10.1126/science.1132588.

Mix, A.C., Pisias, N.G., Rugh, W., Wilson, J., Morey, A., Hagelberg, T.K., Pisias, N.G., Mayer, L.A., Janecek, T.R., Palmer-Julson, A., van Andel, T.H., 1995. Benthic foraminifer stable isotope record from Site 849 (0–5 Ma): local and global climate changes. In: Proceedings of the Ocean Drilling Program, Scientific Results, 138: College Station, TX (Ocean Drilling Program). pp. 371–412. https://doi.org/10.2973/odp.proc.sr.138.120.1995.

Mulitza, S., Rühlemann, C., Bickert, T., Hale, W., Pätzold, J., Wefer, G., 1998. Late Quaternary δ13C gradients and carbonate accumulation in the western equatorial Atlantic. Earth Planet. Sci. Lett. 155 (3–4), 237–249. https://doi.org/10.1016/S0012-821X(98)00012-0.

Murray, R., Knowlton, C., Leinen, M., Mix, A., Polsky, C., 2000. Export production and terrigenous matter in the Central Equatorial Pacific Ocean during interglacial oxygen isotope Stage 11. Glob. Planet. Chang. 24 (1), 59–78. https://doi.org/10.1016/S0921-8181(99)00066-1.

Nakano, H., Tsujino, H., Sakamoto, K., Urakawa, S., Toyoda, T., Yamanaka, G., 2018. Identification of the fronts from the Kuroshio Extension to the Subarctic current using absolute dynamic topographies in satellite altimetry products. J. Oceanogr. 74 (4), 393–420. https://doi.org/10.1007/s10872-018-0470-4.

Nathan, S.A., Leckie, R.M., 2009. Early history of the Western Pacific warm Pool during the middle to late Miocene (~13.2–5.8 Ma): Role of sea-level change and implications for equatorial circulation. Palaeogeogr. Palaeoclimatol. Palaeoecol. 274 (3–4), 140–159. https://doi.org/10.1016/j.palaeo.2009.01.007.

Nürnberg, C.C., Bohrmann, G., Schlüter, M., Frank, M., 1997. Barium accumulation in the Atlantic sector of the Southern Ocean: results from 190,000-year records. Paleoceanography 12 (4), 594–603. https://doi.org/10.1029/97PA01130.

Palter, J.B., Sarmiento, J.L., Gnanadesikan, A., Simeon, J., Slater, R.D., 2010. Fueling export production: nutrient return pathways from the deep ocean and their dependence on the Meridional Overturning Circulation. Biogeosciences 7 (11), 3549–3568. https://doi.org/10.5194/bg-7-3549-2010.

Paytan, A., Griffith, E.M., 2007. Marine barite: Recorder of variations in ocean export productivity. Deep-Sea Res. II Top. Stud. Oceanogr. 54 (5–7), 687–705. https://doi.org/10.1016/j.dsr2.2007.01.007.

Picaut, J., Ioualalen, M., Menkès, C., Delcroix, T., Mcphaden, M.J., 1996. Mechanism of the zonal displacements of the Pacific warm pool: Implications for ENSO. Science 274 (5292), 1486–1489. https://doi.org/10.1126/science.274.5292.1486.

Raddatz, J., Nürnberg, D., Tiedemann, R., Rippert, N., 2017. Southeastern marginal West Pacific warm Pool Sea-surface and thermocline dynamics during the Pleistocene (2.5–0.5 Ma). Palaeogeogr. Palaeoclimatol. Palaeoecol. 471, 144–156. https://doi.org/10.1016/j.palaeo.2017.01.024.

Ravelo, A.C., Fairbanks, R.G., 1995. Carbon isotopic fractionation in multiple species of planktonic foraminifera from core-tops in the tropical Atlantic. Oceanogr. Lit. Rev. 42 (10), 854.

Ravelo, A.C., Hillaire-Marcel, C., 2007. The use of oxygen and carbon isotopes of foraminifera in paleoceanography. In: Hillaire-Marcel, C., De Vernal, A. (Eds.), Proxies in Late Cenozoic Paleoceanography, Developments in Marine Geology Series, Vol. 1. Elsevier, Amsterdam, pp. 735–764. https://doi.org/10.1016/S1572-5480(07)01023-8.

Ravelo, A.C., Fairbanks, R.G., Philander, S.G.H., 1990. Reconstructing tropical Atlantic hydrography using planktonic foraminifera and an ocean model. Paleoceanography 5 (3), 409–431. https://doi.org/10.1029/PA005i003p00409.

Ravelo, A.C., Andreasen, D., Lyle, M.W., Lyle, A.O., Wara, M.W., 2004. Regional climate shifts caused by gradual global cooling in the Pliocene epoch. Nature 429 (6989), 263–267. https://doi.org/10.1038/nature02567.

Ravelo, A.C., Lawrence, K.T., Fedorov, A., Ford, H.L., 2014. Comment on "a 12-million-year temperature history of the tropical Pacific Ocean". Science 346 (6216), 1467. https://doi.org/10.1126/science.1257618.

Regenberg, M., Steph, S., Nurnberg, D., Tiedemann, R., Garbe-Schonberg, D., 2009. Calibrating Mg/Ca ratios of multiple planktonic foraminiferal species with δ18O-calcification temperatures: Paleothermometry for the upper water column. Earth Planet. Sci. Lett. 278 (3–4), 324–336. https://doi.org/10.1016/j.epsl.2008.12.019.

Reghellin, D., Dickens, G.R., Coxall, H.K., Backman, J., 2020. Understanding bulk sediment stable isotope records in the Eastern Equatorial Pacific, from seven million years ago to present day. Paleoceanogr. Paleoclimatol. 35 (2), e2019PA003586. https://doi.org/10.1029/2019PA003586.

Rippert, N., Nürnberg, D., Raddatz, J., Maier, E., Hathorne, E., Bijma, J., Tiedemann, R., 2016. Constraining foraminiferal calcification depths in the western Pacific warm pool. Mar. Micropaleontol. 128, 14–27. https://doi.org/10.1016/j.marmicro.2016.08.004.

Rosenthal, Y., Holbourn, A.E., Kulhanek, D.K., the Expedition 363 Scientists, 2017. Expedition 363 preliminary Report: Western Pacific Warm Pool. Int. Ocean Disc. Prog. https://doi.org/10.14379/iodp.pr.363.2017.

Rosenthal, Y., Holbourn, A.E., Kulhanek, D.K., Aiello, I.W., Babila, T.L., Bayon, G., Beaufort, L., Bova, S.C., Chun, J.-H., Dang, H., Drury, A.J., Dunkley Jones, T., Eichler, P.P.B., Fernando, A.G.S., Gibson, K.A., Hatfield, R.G., Johnson, D.L., Kumagai, Y., Li, T., Linsley, B.K., Meinicke, N., Mountain, G.S., Opdyke, B.N., Pearson, P.N., Poole, C.R., Ravelo, A.C., Sagawa, T., Schmitt, A., Wurtzel, J.B., Xu, J., Yamamoto, M., and Zhang, Y.G., 2018. Site U1490. In Rosenthal, Y., Holbourn, A.E., Kulhanek, D.K., and the Expedition 363 Scientists, Western Pacific Warm Pool. Proceedings of the International Ocean Discovery Program, 363: College Station, TX (International Ocean Discovery Program). Doi:10.14379/iodp.proc.363.111.2018.

Sagawa, T., Yokoyama, Y., Ikehara, M., Kuwae, M., 2012. Shoaling of the western equatorial Pacific thermocline during the last glacial maximum inferred from multispecies temperature reconstruction of planktonic foraminifera. Palaeogeogr. Palaeoclimatol. Palaeoecol. 346–347, 120–129. https://doi.org/10.1016/j.palaeo.2012.06.002.

Sarmiento, J.L., Gruber, N., Brzezinski, M., Dunne, J., 2004. High-latitude controls of thermocline nutrients and low latitude biological productivity. Nature 427 (6969), 56–60. https://doi.org/10.1038/nature02127.

Sarnthein, M., Winn, K., 1990. Reconstruction of Low and Middle Latitude Export Productivity, 30,000 Years BP to Present: Implications for Global Carbon Reservoirs, Climate–Ocean Interaction. Springer, Dordrecht, pp. 319–342. https://doi.org/10.1007/978-94-009-2093-4_16.

Schmidt, H., Berger, W.H., Bickert, T., Wefer, G., 1993. Quaternary carbon isotope record of pelagic foraminifers: Site 806, Ontong Java Plateau. In: Berger, W.H., Kroenke, L.W., Mayer, L.A., et al. (Eds.), Proceedings of the Ocean Drilling Program, Scientific Results, 130. Ocean Drilling Program, College Station, TX, pp. 397–409. https://doi.org/10.2973/odp.proc.sr.130.024.1993.

Schneider, B., Schmittner, A., 2006. Simulating the impact of the Panamanian seaway closure on ocean circulation, marine productivity and nutrient cycling. Earth Planet. Sci. Lett. 246 (3), 367–380. https://doi.org/10.1016/j.epsl.2006.04.028.

Schneider, T., Bischoff, T., Haug, G.H., 2014. Migrations and dynamics of the intertropical convergence zone. Nature 513 (7516), 45–53. https://doi.org/10.1038/nature13636.

Shankle, M.G., Burls, N.J., Fedorov, A.V., Thomas, M.D., Liu, W., Penman, D.E., Ford, H.L., Jacobs, P.H., Planavsky, N.J., Hull, P.M., 2021. Pliocene decoupling of equatorial Pacific temperature and pH gradients. Nature 598 (7881), 457–461. https://doi.org/10.1038/s41586-021-03884-7.

Steinke, S., Mohtadi, M., Groeneveld, J., Lin, L.C., Löwemark, L., Chen, M.T., Rendle-Bühring, 2010. Reconstructing the southern South China Sea upper water column structure since the last Glacial Maximum: Implications for the East Asian winter monsoon development. Paleoceanography 25 (2). https://doi.org/10.1029/2009PA001850.

Steph, S., Tiedemann, R., Groeneveld, J., Sturm, A., Nürnberg, D., 2006. Pliocene changes in tropical East Pacific upper ocean stratification: response to tropical gateways? In: Tiedemann, R., Mix, A.C., Richter, C., Ruddiman, W.F. (Eds.), Proceedings of the Ocean Drilling Program, Scientific Results, 202. Ocean Drilling Program, College Station, TX, pp. 1–51. https://doi.org/10.2973/odp.proc.sr.202.211.2006.

Steph, S., Tiedemann, R., Prange, M., Groeneveld, J., Schulz, M., Timmermann, A., Nürnberg, D., Rühlemann, C., Saukel, C., Haug, G.H., 2010. Early Pliocene increase in thermohaline overturning: a precondition for the development of the modern equatorial Pacific cold tongue. Paleoceanography 25 (2). https://doi.org/10.1029/2008PA001645.

Tiedemann, R., Sturm, A., Steph, S., Lund, S.P., Stoner, J.S., 2007. Astronomically calibrated timescales from 6 to 2.5 Ma and benthic isotope stratigraphies, Sites 1236, 1237, 1239, and 1241. In: Tiedemann, R., Mix, A.C., Richter, C., Ruddiman, W.F. (Eds.), Proceedings of the Ocean Drilling Program, Scientific Results, 202. Ocean Drilling Program, College Station, TX, pp. 1–69. https://doi.org/10.2973/odp.proc.sr.202.210.2007.

Toggweiler, J.R., Dixon, K., Broecker, W.S., 1991. The Peru upwelling and the ventilation of the South Pacific thermocline. J. Geophys. Res. Oceans 96 (C11), 20467–20497. https://doi.org/10.1029/91JC02063.

Toole, J., Zou, E., Millard, R., 1988. On the circulation of the upper waters in the western equatorial Pacific Ocean. Deep Sea Res. Part A. Ocean. Res. Papers 35 (9), 1451–1482. https://doi.org/10.1016/0198-0149(88)90097-0.

Turk, D., Lewis, M.R., Harrison, G.W., Kawano, T., Asanuma, I., 2001. Geographical distribution of new production in the western/central equatorial Pacific during El Niño and non-El Niño conditions. J. Geophys. Res. Oceans 106 (C3), 4501–4515. https://doi.org/10.1029/1999JC000058.

Wara, M.W., Ravelo, A.C., Delaney, M.L., 2005. Permanent El Niño-like conditions during the Pliocene warm period. Science 309 (5735), 758–761. https://doi.org/10.1126/science.1112596.

Wells, M.L., Vallis, G.K., Silver, E.A., 1999. Tectonic processes in Papua New Guinea and past productivity in the eastern equatorial Pacific Ocean. Nature 398 (6728), 601–604. https://doi.org/10.1038/19281.

Willeit, M., Ganopolski, A., Calov, R., Robinson, A., Maslin, M., 2015. The role of CO_2 decline for the onset of Northern Hemisphere glaciation. Quat. Sci. Rev. 119, 22–34. https://doi.org/10.1016/j.quascirev.2015.04.015.

Williams, B., Grottoli, A.G., 2010. Recent shoaling of the nutricline and thermocline in the western tropical Pacific. Geophys. Res. Lett. 37 (22). https://doi.org/10.1029/2010GL044867.

Wu, G., Berger, W.H., 1991. Pleistocene $\delta^{18}O$ records from Ontong-Java Plateau: Effects of winnowing and dissolution. Mar. Geol. 96 (3), 193–209. https://doi.org/10.1016/0025-3227(91)90147-V.

Yamasaki, M., Sasaki, A., Oda, M., Domitsu, H., 2008. Western equatorial Pacific planktic foraminiferal fluxes and assemblages during a La Niña year (1999). Mar. Micropaleontol. 66 (3–4), 304–319. https://doi.org/10.1016/j.marmicro.2007.10.006.

Yan, X.-H., Ho, C.-R., Zheng, Q., Klemas, V., 1992. Temperature and size variabilities of the Western Pacific warm Pool. Science 258 (5088), 1643–1645. https://doi.org/10.1126/science.258.5088.1643.

Zenk, W., Siedler, G., Ishida, A., Holfort, J., Kashino, Y., Kuroda, Y., Miyama, T., Müller, T.J., 2005. Pathways and variability of the Antarctic Intermediate Water in the western equatorial Pacific Ocean. Prog. Oceanogr. 67 (1–2), 245–281. https://doi.org/10.1016/j.pocean.2005.05.003.

Zweng, M.M., Reagan, J.R., Antonov, J.I., Locarnini, R.A., Mishonov, A.V., Boyer, T.P., Garcia, H.E., Baranova, O.K., Johnson, D.R., Seidov, D., Biddle, M.M., 2013. World Ocean Atlas 2013. In: Levitus, S. (Ed.), Salinity, Vol. 2, p. 39 Mishonov, A. Technical Ed.; NOAA Atlas NESDIS 74 https://doi.org/10.7289/V5251G4D.